

# Predictive variational inference for flexible regression models

Lucas Kock<sup>1</sup>, Scott A. Sisson<sup>2</sup>, G. S. Rodrigues<sup>3</sup>, and David J. Nott<sup>1</sup>

## Abstract

A conventional Bayesian approach to prediction uses the posterior distribution to integrate out parameters in a density for unobserved data conditional on the observed data and parameters. When the true posterior is intractable, it is replaced by an approximation; here we focus on variational approximations. Recent work has explored methods that learn posteriors optimized for predictive accuracy under a chosen scoring rule, while regularizing toward the prior or conventional posterior. Our work builds on an existing predictive variational inference (PVI) framework that improves prediction, but also diagnoses model deficiencies through implicit model expansion. In models where the sampling density depends on the parameters through a linear predictor, we improve the interpretability of existing PVI methods as a diagnostic tool. This is achieved by adopting PVI posteriors of Gaussian mixture form (GM-PVI) and establishing connections with plug-in prediction for mixture-of-experts models. We make three main contributions. First, we show that GM-PVI prediction is equivalent to plug-in prediction for certain mixture-of-experts models with covariate-independent weights in generalized linear models and hierarchical extensions of them. Second, we extend standard PVI by allowing GM-PVI posteriors to vary with the prediction covariate and in this case an equivalence to plug-in prediction for mixtures of experts with covariate-dependent weights is established. Third, we demonstrate the diagnostic value of this approach across several examples, including generalized linear models, linear mixed models, and latent Gaussian process models, demonstrating how the parameters of the original model must vary across the covariate space to achieve improvements in prediction.

**Keywords:** generalized Bayes, generalised linear models, mixture models, posterior predictive, predictively oriented posteriors, variational Bayes

**Acknowledgments:** SAS is supported by the Australian Research Council through the Discovery Project program (DP260101134). David Nott's research was supported by the Ministry of Education, Singapore, under the Academic Research Fund Tier 2 (MOE-T2EP20123-0009), and he is affiliated with the Institute of Operations Research and Analytics at the National University of Singapore.

<sup>1</sup> Department of Statistics and Data Science, National University of Singapore, Singapore; lucas.kock@nus.edu.sg, standj@nus.edu.sg

<sup>2</sup> School of Mathematics and Statistics, University of New South Wales, Australia; scott.sisson@unsw.edu.au

<sup>3</sup> Department of Statistics, University of Brasília, Brazil; guilhermerodrigues@unb.br

# 1 Introduction

It is well-known that Bayesian inference can perform poorly in situations where the model is misspecified. Bayesian inference about the parameters can become meaningless under misspecification (Walker; 2013), and Bayesian prediction can only be defended as optimal when the model is correct (Aitchison; 1975). A growing literature has proposed modifications to conventional Bayesian predictive inference with improved performance under misspecification. Some of these modifications simultaneously pursue another goal: providing insight into how the model can be improved. The idea is that an expanded model could recover the predictive gains offered by the modified predictive approach for the original model, but in a conventional Bayesian way. This paper focuses on so-called predictive variational inference (PVI) methods (e.g. Lai and Yao; 2024). In PVI methods, a PVI posterior is learnt on the parameters by optimizing a criterion that leads to good prediction when parameters are integrated out using the PVI posterior in forming predictive distributions. We focus here on obtaining interpretable PVI posteriors that can guide model improvement.

To attain the goal of good prediction under misspecification which is informative for model expansion, we consider regression models where the sampling density for a new observation depends on the unknown parameters through a scalar linear predictor. Common models satisfying this requirement include generalized linear models, their hierarchical extensions, and latent Gaussian process models. We consider Gaussian mixture PVI approximations, and using the assumed structure of the model we can compute predictive densities using only one-dimensional quadrature. These predictive densities are themselves mixtures, which follows from the Gaussian mixture PVI (GM-PVI) posterior form. We make three main contributions. First, we establish a connection between GM-PVI posterior prediction and mixture-of-experts model expansions with covariate-independent weights. Second, we establish an analogous connection for mixture-of-experts expansions with covariate-dependent weights, enabled by a novel extension in which the GM-PVI posterior is allowed to vary with the prediction covariate. This yields what we call varying GM-PVI (VGM-PVI) posteriors. Third, through a range of examples, we show that the mixture-of-experts connection provides insight into model deficiencies, demonstrating how the parameters must change across the covariate space to improve prediction. The most important contribution is the second one: allowing the PVI posterior to depend on co-

variates in regression settings. Our examples demonstrate that VGM-PVI substantially enhances the utility of PVI as a tool for model criticism.

Our work is most closely related to that of Lai and Yao (2024), although other related approaches are discussed below. In their PVI approach, Lai and Yao (2024) consider a parametrized form for a posterior approximation, but instead of approximating the conventional posterior distribution, which may not be desirable under model misspecification, they optimize predictive performance of the PVI posterior according to a scoring rule. In the optimization, they regularize the PVI posterior either towards the prior or conventional posterior. Their work is motivational for ours in their focus on diagnosing misspecification, and their interpretation of PVI as an implicit model expansion which can be insightful for model improvement. In particular, they consider the change in variability between the PVI posterior and conventional posterior as suggestive of which parameters in the current model need to vary across observations to achieve a better model. Lai and Yao (2024) describe methods for implementing PVI for several different scoring rules, and also in the context of likelihood-free or simulation-based inference (Sisson et al.; 2018; Cranmer et al.; 2020). The method of Lai and Yao (2024) can be thought of as a continuous version of Bayesian model stacking (Yao et al.; 2018), where a density on parameters is optimized for prediction rather than a set of weights for a discrete set of models. In this analogy, our novel extension of PVI posteriors allowing them to vary with prediction covariates is analogous to hierarchical model stacking (Yao et al.; 2022).

Recent work of McLatchie et al. (2025) provides the most comprehensive theoretical analysis of predictive variational and related predictively oriented Bayesian methods to date. They define a PRO posterior as a solution to an optimization problem where the objective incorporates a scoring rule term and a term regularizing towards the prior. McLatchie et al. (2025) prove some results concerning the behaviour of the PRO posterior relative to a Gibbs posterior based on the same scoring rule. One of these shows that under correct model specification the PRO posterior achieves the same predictive performance as the corresponding Gibbs posterior, while in non-trivial misspecified settings it is strictly superior in terms of the divergence induced by the scoring rule. They devise algorithms for computing PRO posteriors using a mean-field Langevin dynamics approach; Chazal et al. (2025) discuss alternative computational methods that may require less tuning. McLatchie

et al. (2025, Section 4.2.2) also discuss the relationship of the PRO posterior to mixture models for the data, which is relevant to our current work. Our approach differs, however, in adopting a finite mixture form for the PVI posterior itself.

Also relevant to our work is research on generalized Bayes and generalized variational inference (Knoblauch et al.; 2022) and PAC-Bayesian bounds (Alquier; 2024). Masegosa (2020) emphasizes the difference between inferential and predictive risk, and bound the latter using second-order PAC-Bayesian bounds. Their sharper bounds lead to improved predictive performance according to the log score, and contain a diversity term that provides a novel interpretation of why diverse ensembles are beneficial in ensemble learning. Related work of Morningstar et al. (2022) develops PAC<sup>m</sup>-Bayes, giving a multi-sample bound for predictive risk based on the log score which becomes tight as the sample size tuning parameter  $m$  in the bound increases. We also focus on the log score in our work, but in situations where the log score can be computed in closed form, or accurately computed using one-dimensional quadrature. Shen et al. (2025) consider an approach to uncertainty quantification in misspecified deterministic models, where predictive distributions are formed by placing a mixing distribution on the model parameters. They consider a generalized variational inference criterion involving a maximum mean discrepancy between the variational predictive and the empirical distribution of the data, together with a regularization term involving Kullback-Leibler divergence between the mixing distribution and the prior. Their work is novel in considering uncertainty quantification for deterministic models, but this will not be our focus here.

A number of authors have considered generalized variational inference approaches to improve prediction in the particular context of sparse Gaussian processes (GPs; Titsias; 2009) and related models. Jankowiak et al. (2020) considers the form of the predictive distribution arising in sparse GPs and define a parametric model motivated by this, optimizing parameters directly based on a log score with a regularization term. Jankowiak et al. (2020) considers a related approach, where a so-called deep sigma point process (DSPP) model is defined, motivated by the form of the predictive distribution for a deep Gaussian process. The DSPP model replaces continuous mixing in the deep GP approach with a finite mixture based on quadrature approximations. The quadrature points and weights are free parameters which are optimized for predictive performance along with

other parameters by regularized maximum likelihood. The predictive distribution has the form of a Gaussian mixture, which we also consider here, but we focus on different types of models and also consider variational posteriors which vary according to the covariate at which prediction is required. Several authors consider direct loss minimization for sparse Gaussian processes, where the direct loss is the log score. Sheth and Khardon (2020) derive risk bounds which apply for a smoothed log loss in sparse GP regression. Wei et al. (2021) focuses on computational issues, addressing the issue of gradient estimation for direct loss minimization.

There are many novel recent developments in Bayesian prediction broadly, and we refer the reader to a recent special issue in the journal *Statistical Science* for an excellent overview (Clarke and Rigo; 2025). Since we focus on PVI methods which are interpretable for model expansion, our work is also related to Bayesian predictive model checking (see, for example, Gelman et al. 1996 and Evans 2015, Chapter 5). However, the PVI methods here are different to conventional model checking approaches in focusing on modifying prediction in an existing model to obtain better predictions in addition to understanding misspecification.

In the next section, we provide background on variational inference and Bayesian predictive inference. Section 3 develops PVI with a Gaussian mixture variational family, establishing connections with plug-in prediction for mixture-of-experts models, and introduces VGM-PVI posteriors that vary with the prediction covariates, linking them to mixture-of-experts expansions with covariate-dependent weights. Sections 4 through 6 present examples. Section 4 considers linear, logistic, and Poisson regression, Section 5 considers hierarchical models with random effects and Section 6 considers latent Gaussian process models. Section 7 gives concluding discussion. Code is publicly available at [github.com/kocklucx/GMPVI](https://github.com/kocklucx/GMPVI).

## 2 Background

Suppose we have a statistical model with parameters  $\theta \in \Theta$  for data  $y = (y_1, \dots, y_n)^\top \in \mathcal{Y}^n$ . We adopt a Bayesian approach to learning about  $\theta$ , using a prior density  $p(\theta)$ . Regression problems are considered where  $y$  is a vector of responses, and for each  $y_i$  there is an associated covariate  $x_i = (x_{i1}, \dots, x_{ip})^\top \in \mathcal{X}$ . We write  $X = \{x_1, \dots, x_n\}$ . The covariates  $X$  are

not modelled, but only  $y|X$ . The sampling density of  $y|X, \theta$  is  $p(y|X, \theta)$ , but henceforth we generally write this as  $p(y|\theta)$  for simplicity. The posterior density is  $p(\theta|y) \propto p(\theta)p(y|\theta)$ . Similar to our notation for the sampling density, we suppress dependence on covariates in our notation for posterior densities and predictive densities, except where showing the dependence explicitly is necessary for clarity.

In Bayesian inference we need to summarize the posterior distribution, and variational inference (VI; Blei et al.; 2017) is one method to do this. It optimizes a posterior approximation in a convenient class of densities which we denote as  $\mathcal{Q} = \{q_\lambda(\theta); \lambda \in \Lambda\}$ , where  $\lambda$  is a vector of variational parameters. A commonly used measure of the quality of a variational approximation is the Kullback-Leibler (KL) divergence, and in this case the approximate posterior density is  $q_{\lambda^*}(\theta)$ , where

$$\lambda^* = \arg \min_{\lambda \in \Lambda} \text{KL}(q_\lambda(\theta) || p(\theta|y)), \quad (1)$$

and

$$\text{KL}(q_\lambda(\theta) || p(\theta|y)) = \int q_\lambda(\theta) \log \frac{q_\lambda(\theta)}{p(\theta|y)} d\theta. \quad (2)$$

We have assumed a unique minimizer  $\lambda^*$ . The optimization (1) is equivalent to maximization of the so-called evidence lower bound (ELBO; Ormerod and Wand; 2010),

$$\lambda^* = \arg \max_{\lambda \in \Lambda} \text{ELBO}(\lambda), \quad (3)$$

where  $\text{ELBO}(\lambda) := \mathbb{E}_q[\log p(\theta)p(y|\theta) - \log q_\lambda(\theta)]$  and  $\mathbb{E}_q[\cdot]$  denotes expectation with respect to  $q_\lambda(\theta)$ . The ELBO gets its name as a lower bound on the evidence  $\log p(y)$ , where

$$p(y) = \int p(\theta)p(y|\theta) d\theta.$$

The ELBO is convenient to work with in optimization because its expression does not involve any unknown posterior normalizing constant.

Let  $\tilde{y}$  denote an unobserved response with observed covariate  $\tilde{x} \in \mathcal{X}$ , and suppose the model for  $\tilde{y}|\tilde{x}$  is  $p(\tilde{y}|\tilde{x}, \theta)$ . In traditional Bayesian inference, the predictive density for  $\tilde{y}|\tilde{x}, y$  is

$$p(\tilde{y}|\tilde{x}, y) = \int p(\tilde{y}|\tilde{x}, \theta)p(\theta|y) d\theta, \quad (4)$$

where it is assumed here that  $\tilde{y}$  and  $y$  are conditionally independent given  $\theta$  and the covariates. The PVI approach of Lai and Yao (2024) replaces the posterior distribution in the integrand in (4) with a PVI posterior  $q_\lambda(\theta) \in \mathcal{Q}$ , to construct a predictive density as

$$q_\lambda(\tilde{y}|\tilde{x}) := \int p(\tilde{y}|\tilde{x}, \theta) q_\lambda(\theta) d\theta. \quad (5)$$

PVI chooses  $\lambda$  so that the predictions obtained by (5) are optimal according to some chosen scoring rule. Some background on scoring rules is given now; this is necessary so that the objective function used to choose  $\lambda$  in PVI can be explained.

Let  $\mathcal{P}$  be a space of distributions for data  $z \in \mathcal{Y}$  to be observed. A scoring rule is a function  $\mathcal{S} : \mathcal{P} \times \mathcal{Y} \rightarrow \overline{\mathbb{R}}$ , where  $\overline{\mathbb{R}} = \mathbb{R} \cup \{-\infty, \infty\}$ . For data  $z$  and  $P \in \mathcal{P}$ , we think of  $S(P, z)$  as a measure of consistency of the data  $z$  with the distribution  $P$ . We will define scoring rules so that a larger value means greater consistency (so-called positively-oriented scoring rules). If  $P, Q \in \mathcal{P}$ , we use a common abuse of notation and write  $S(P, Q) := \mathbb{E}_{Z \sim Q}(S(P, Z))$ . A scoring rule is proper for  $\mathcal{P}$  if  $S(P, P) \geq S(P, Q)$  for any  $Q \in \mathcal{P}$ . It is strictly proper for  $\mathcal{P}$  if  $S(P, P') \geq S(P, Q)$  for all  $Q \in \mathcal{P}$  implies that  $P = P'$ . If  $P$  and  $Q$  have densities  $p(\cdot)$  and  $q(\cdot)$  say, we will also write  $S(p(\cdot), z) := S(P, z)$  and  $S(p(\cdot), q(\cdot)) := S(P, Q)$ . For further background on scoring rules, see Gneiting and Raftery (2007).

For a given scoring rule, we can define the objective optimized in PVI as follows. We change the optimization problem (1) to

$$\lambda^* = \arg \max_{\lambda} \left\{ \sum_{i=1}^n S(q_\lambda(\cdot|x_i), y_i) - \beta \cdot \text{KL}(q_\lambda(\theta) || p(\theta|y)) \right\}, \quad (6)$$

where  $\beta > 0$  is a tuning parameter. Then  $q_{\lambda^*}(\tilde{y}|\tilde{x})$  is the predictive density for future data  $\tilde{y}$  given  $\tilde{x}$ . To interpret (6), observe that the first term,  $\sum_{i=1}^n S(q_\lambda(\cdot|x_i), y_i)$ , is a measure of how well the predictive densities  $q_\lambda(\cdot|x_i)$  predict the observed data. The second term in (6) is a regularization, encouraging the pseudo-posterior to be close to the actual posterior density. Lai and Yao (2024) observe that  $\text{KL}(q_\lambda(\theta) || p(\theta|y))$  can be replaced by something else, but we use the formulation in (6) here. As  $\beta \rightarrow \infty$  the regularizer dominates the objective function, so that optimizing (6) becomes the same as ordinary variational inference optimizing the ELBO. An equivalent form of the optimization (6) is

$$\lambda^* = \arg \max_{\lambda} \left\{ \sum_{i=1}^n S(q_\lambda(\cdot|x_i), y_i) + \beta \cdot \text{ELBO}(\lambda) \right\}. \quad (7)$$

Lai and Yao (2024) consider various possibilities for the scoring rule used in (6), including the log score and the continuous ranked probability score. Here we use the log score, i.e.  $S(q_\lambda(\cdot), y_i) = \log q_\lambda(y_i)$ .

### 3 Gaussian mixture PVI posteriors

Gaussian mixture PVI posteriors for generalized linear models are discussed in this section. Hierarchical extensions are developed later in Section 5.

#### 3.1 PVI for generalized linear models

Consider a Gaussian mixture PVI (GM-PVI) posterior of the form

$$q_\lambda(\theta) = \sum_{k=1}^K \omega_k \phi(\theta; \mu_k, \Sigma_k), \quad (8)$$

where  $\omega_k \geq 0$  are mixing weights,  $\sum_{k=1}^K \omega_k = 1$ , and  $\phi(\theta; \mu_k, \Sigma_k)$  is a multivariate normal density with mean  $\mu_k$  and covariance matrix  $\Sigma_k$ . Write  $\omega = (\omega_2, \dots, \omega_K)^\top$  with  $\omega_1 = 1 - \sum_{k=2}^K \omega_k$ ,  $\mu = (\mu_1^\top, \dots, \mu_K^\top)^\top$  and  $\gamma = (\text{vech}(\Sigma_1)^\top, \dots, \text{vech}(\Sigma_K)^\top)^\top$ , where  $\text{vech}(A)$  for a square matrix  $A$  is the vector obtained by stacking lower-triangular elements of  $A$  columnwise left to right. The vector of variational parameters in our GM-PVI is  $\lambda = (\omega^\top, \mu^\top, \gamma^\top)^\top$ .

It is helpful to begin with a simple case, a linear model:

$$y_i = x_i^\top \theta + \epsilon_i, \quad \epsilon_i \sim N(0, \sigma^2),$$

where  $\sigma^2$  is considered fixed for now. The GM-PVI posterior  $q_\lambda(\theta)$  leads to the predictive density

$$\begin{aligned} q_\lambda(\tilde{y}|\tilde{x}) &= \int p(\tilde{y}|\tilde{x}, \theta) q_\lambda(\theta) d\theta \\ &= \int \sum_{k=1}^K \omega_k \phi(\theta; \mu_k, \Sigma_k) \phi(\tilde{y}|\tilde{x}^\top \theta, \sigma^2) d\theta \\ &= \sum_{k=1}^K \omega_k \phi(\tilde{y}; \tilde{x}^\top \mu_k, \tilde{x}^\top \Sigma_k \tilde{x} + \sigma^2). \end{aligned} \quad (9)$$

Prediction using (9) is “plug-in” prediction for a mixture of (heteroscedastic) linear regression models, and if the log score is used in PVI, the parameters  $\lambda$  that are plugged

in are being estimated by fitting to the training data using regularized maximum likelihood (7). The information from the prior distribution on  $\theta$  is used in the regularization term, where  $q_\lambda(\theta)$  is encouraged to be close to the posterior, which in turn depends on the prior. Although we assumed  $\sigma^2$  was known, this could also be estimated from the data to optimize predictive performance along with  $\lambda$ . We can also absorb  $\sigma^2$  into  $\theta$ , but then integrating out  $\theta$  can no longer be done in closed form. An example where we do so is given in Supplementary Information B.2. The regression components in the mixture model are heteroscedastic linear regressions, with the form of the variance model a special case of the approach considered in Hoff and Niu (2012).

Next, we expand this mixture of regression interpretation of PVI to generalized linear models (GLMs). For the moment we consider the case where any dispersion parameters are known. Writing  $\mu_i$  for the mean of  $y_i$ , it is assumed that  $g(\mu_i) = x_i^\top \theta$ , for some link function  $g(\cdot)$ . The sampling density for a future response is a function of  $\theta$  only through  $\tilde{x}^\top \theta$ , and we write it as  $p(\tilde{y}|\tilde{x}^\top \theta)$ . If we use the GM-PVI form (8), and write the implied density of  $\tilde{x}^\top \theta$  as

$$q_\lambda(\tilde{x}^\top \theta) = \sum_{k=1}^K \omega_k \phi(\tilde{x}^\top \theta; \tilde{x}^\top \mu_k, \tilde{x}^\top \Sigma_k \tilde{x}),$$

then the GM-PVI predictive density is

$$\begin{aligned} q_\lambda(\tilde{y}|\tilde{x}) &= \int p(\tilde{y}|\tilde{x}^\top \theta) q_\lambda(\tilde{x}^\top \theta) d(\tilde{x}^\top \theta) \\ &= \sum_{k=1}^K \omega_k \int p(\tilde{y}|\tilde{x}^\top \theta) \phi(\tilde{x}^\top \theta; \tilde{x}^\top \mu_k, \tilde{x}^\top \Sigma_k \tilde{x}) d(\tilde{x}^\top \theta). \end{aligned} \quad (10)$$

Denote the integral in the  $k$ th term of (10) as

$$I_k = \int p(\tilde{y}|\tilde{x}^\top \theta) \phi(\tilde{x}^\top \theta; \tilde{x}^\top \mu_k, \tilde{x}^\top \Sigma_k \tilde{x}) d(\tilde{x}^\top \theta).$$

If we consider a change of variable

$$w = \frac{\tilde{x}^\top \theta - \tilde{x}^\top \mu_k}{\sqrt{\tilde{x}^\top \Sigma_k \tilde{x}}}$$

so that  $\tilde{x}^\top \theta = \tilde{x}^\top \mu_k + w\sqrt{\tilde{x}^\top \Sigma_k \tilde{x}}$ , we obtain

$$I_k = \int p\left(\tilde{y}|\tilde{x}^\top \mu_k + w\sqrt{\tilde{x}^\top \Sigma_k \tilde{x}}\right) \phi(w; 0, 1) dw,$$

showing that the integrand is a function  $f_k(w)$  multiplied by a standard normal density, so that the integral can be approximated accurately using Gauss-Hermite quadrature (e.g.

Särkkä and Svensson; 2023, Section 8.3) with only a small number of quadrature points. Using  $B$  quadrature points gives exact answers when  $f_k(w)$  is any polynomial up to degree  $2B - 1$ . With this approach we obtain the approximation

$$I_k \approx \sum_{b=1}^B \gamma_{b \cdot p} \left( \tilde{y} | \tilde{x}^\top \mu_k + w_b \sqrt{\tilde{x}^\top \Sigma_k \tilde{x}} \right).$$

where  $\gamma_b \geq 0$ ,  $b = 1, \dots, B$ , are quadrature weights summing to 1, and  $w_b$ ,  $b = 1, \dots, B$ , are the quadrature points. Putting this together with (10), we obtain

$$q_\lambda(\tilde{y} | \tilde{x}) \approx \sum_{k=1}^K \sum_{b=1}^B \omega_k \gamma_{b \cdot p} \left( \tilde{y} | \tilde{x}^\top \mu_k + w_b \sqrt{\tilde{x}^\top \Sigma_k \tilde{x}} \right). \quad (11)$$

The representation (11) demonstrates that the GM-PVI posterior can be approximated by plug-in predictive inference based on a mixture of GLM's with offset terms which are independent of the coefficients  $\mu_k$ . The PVI variational parameters  $\lambda$  are estimated by regularized maximum likelihood, similar to the linear model case. Similar to linear models, if there are any unknown dispersion parameters, these could also be estimated to maximize predictive accuracy. In the case of the linear model, the above representation is not equivalent to the one discussed previously – (11) would be a mixture of homoscedastic linear models, not heteroscedastic models as in (9).

### 3.2 PVI with covariate-dependent GM-PVI's

Next we consider an extension where a GM-PVI is allowed to depend on the prediction covariate, denoted  $\tilde{x}$  here, resulting in what we call varying GM-PVI posteriors (VGM-PVI posteriors). In the VGM-PVI posteriors, we allow the mixing weights in a GM-PVI posterior to vary with  $\tilde{x}$ :

$$\mathcal{Q} = \{q_\lambda(\theta | \tilde{x}) : q_\lambda(\theta | \tilde{x}) = \sum_{k=1}^K \omega_k(\tilde{x}) \phi(\theta; \mu_k, \Sigma_k)\},$$

where

$$\omega_k(\tilde{x}) = \frac{\exp(\tilde{x}^\top \eta_k)}{\sum_{l=1}^K \exp(\tilde{x}^\top \eta_l)},$$

with  $\eta_1 = 0$  for identifiability.

Let's consider first the linear model setting of the previous section. For the VGM-PVI

we obtain

$$\begin{aligned}
q_\lambda(\tilde{y}|\tilde{x}) &= \int p(\tilde{y}|\tilde{x}, \theta) q_\lambda(\theta|\tilde{x}) d\theta \\
&= \int \sum_{k=1}^K w_k(\tilde{x}) \phi(\theta; \mu_k, \Sigma_k) \phi(\tilde{y}|\tilde{x}^\top \theta, \sigma^2) d\theta \\
&= \sum_{k=1}^K \omega_k(\tilde{x}) \phi(\tilde{y}; \tilde{x}^\top \mu_k, \tilde{x}^\top \Sigma_k \tilde{x} + \sigma^2).
\end{aligned} \tag{12}$$

This is similar to (9), with the mixing weights changing from constant to covariate dependent. Similarly in the GLM case we obtain analogous to (11)

$$q_\lambda(\tilde{y}|\tilde{x}^\top \theta) \approx \sum_{k=1}^K \sum_{b=1}^B \omega_k(\tilde{x}) \gamma_{b \cdot p}(\tilde{y}|\tilde{x}^\top \mu_k + w_b \sqrt{\tilde{x}^\top \Sigma_k \tilde{x}}). \tag{13}$$

So again we obtain some equivalences between VGM-PVI posteriors and plug-in prediction for mixture of experts models, but now with covariate-dependent mixture weights.

An additional aspect of VGM-PVI posteriors is that we need to decide what the regularization term in the PVI objective function should be. Here we suggest to use the KL divergence between

$$\bar{q}_\lambda(\theta) = \frac{1}{n} \sum_{i=1}^n q_\lambda(\theta|x_i) = \sum_{k=1}^K \bar{\omega}_k \phi(\theta; \mu_k, \Sigma_k)$$

and  $p(\theta|y)$ . The KL divergence term in the regularizer becomes equivalent to the ordinary ELBO for the density  $\bar{q}_\lambda(\theta)$  for optimization purposes. The density  $\bar{q}_\lambda(\theta)$  is a Gaussian mixture, where the mixing weights,  $\bar{\omega}_k = n^{-1} \sum_{i=1}^n \omega_k(x_i)$ , are the average of the mixing weights in the  $q_\lambda(\theta|x_i)$ . However, there are many alternative ways we can obtain a set of average PVI posteriors over covariates close to the true posterior. The regularizer becomes

$$\begin{aligned}
&\sum_{k=1}^K \bar{\omega}_k \mathbb{E}_{\phi(\theta; \mu_k, \Sigma_k)} [\log p(y | \theta) + \log p(\theta)] + \mathbb{E}_{\bar{q}_\lambda(\theta)} [-\log \bar{q}_\lambda(\theta)] \\
&= \sum_{k=1}^K n^{-1} \sum_{i=1}^n \mathbb{E}_{\phi(\theta; \mu_k, \Sigma_k)} [\omega_k(x_i) \log (p(y_i | \theta)p(\theta))] + \mathbb{E}_{\bar{q}_\lambda(\theta)} [-\log \bar{q}_\lambda(\theta)].
\end{aligned}$$

So the regularizer encourages the ‘‘average PVI posterior’’ to be close to the posterior. In particular, the first term forces each mixture component to be close to the weighted posterior for the sub-data in the region on which the component is actually active. For the expected log-likelihood terms, expectations are only taken over single Gaussians, so that these terms can be derived in closed form for many common GLMs. Alternatively, similar to the computation of the predictive densities  $q_\lambda(y_i|x_i)$ , Gauss-Hermite quadrature can be

employed. The second term acts as a global penalty for the complexity of the mixture model in terms of its entropy. This depends only on the Gaussian mixture density  $\bar{q}(\theta)$ , and we use a closed-form approximation for entropy of Gaussian mixtures given in Huber et al. (2008). We give analytic expressions for the optimization targets for all examples considered within the manuscript in Supplementary Information A.

To ensure positive definiteness of the mixture covariance matrices,  $\Sigma_k$ , we consider the Cholesky decomposition  $\Sigma_k = C_k C_k^\top$  with a lower triangular matrix  $C_k$  with positive diagonal. Writing  $A^*$  for any matrix  $A$ , such that  $A_{ij}^* = A_{ij}$  if  $i \neq j$  and  $A_{jj}^* = \log A_{jj}$ , the non-zero entries of  $C_k^*$  are unrestricted. Writing  $\eta = (\eta_2^\top, \dots, \eta_K^\top)^\top$ ,  $\mu = (\mu_1^\top, \dots, \mu_K^\top)^\top$ , and  $c = (\text{vech}(C_1^*)^\top, \dots, \text{vech}(C_K^*)^\top)^\top$ , the vector of variational parameters in VGM-PVI is  $\lambda = (\eta^\top, \mu^\top, c^\top)^\top$ . Due to the closed form of the optimization target,  $\lambda$  is optimized using a simple gradient ascent (GA) scheme with the adaptive Adam learning rate (Kingma and Ba; 2014).

A particular challenge when working with mixture models is selecting the number of mixture components. In the examples discussed below the number of mixture components is chosen along the following heuristic. We initialize GA with a large number of potential components set to  $K = 10$  for the GLM examples, and to  $K = 5$  in all other examples. After 2,000 steps of GA all components  $k$  for which  $\omega_k(x_i) < \omega_l(x_i)$  for all  $i = 1, \dots, n$ ,  $l \neq k$ , are removed from the model. This procedure is repeated until no further components are removed and the algorithm is then run until convergence. Even though there is no theoretical guarantee that this heuristic results in an optimal choice for  $K$ , we found this to be a fast way of selecting a reasonable model in all examples considered. Alternatively, models for several choices of  $K$  can be trained and the best one can then be selected based on some model selection criterion. The recent work by Davies et al. (2025) could also be adapted to perform predictive variational model averaging.

## 4 Experiments and Applications

This section illustrates VGM-PVI in several GLM tasks. An additional simulation study and an example with a Gaussian likelihood model are given in Supporting Information B.1 and B.2 respectively.

## 4.1 Simulations – Logistic classification

As a first example, we consider a synthetic binary classification task from McLatchie et al. (2025). For  $i = 1, \dots, n$ , covariates  $x_i$  are uniformly drawn on  $[-2, 2]^2$ , and labels  $y_i$  are deterministically assigned to data in the top-left and the bottom-right quadrant, while labels in the remaining two quadrants are assigned randomly. That is

$$y_i | x_i \sim \begin{cases} \text{Bern}(0) & \text{if } x_{i1} < 0, x_{i2} > 0; \\ \text{Bern}(1) & \text{if } x_{i1} > 0, x_{i2} < 0; \\ \text{Bern}(0.5) & \text{else,} \end{cases}$$

where  $\text{Bern}(p)$  denotes the Bernoulli distribution with success probability  $p$ . We train a logistic regression model  $y_i \sim \text{Bern}(\sigma(x_i^\top \theta))$  with prior  $\theta \sim \mathcal{N}(0, 2.5^2 I_2)$ , where  $\sigma(\cdot)$  denotes the logistic function, to a data set with  $n = 1,000$  observations. Predictions based on the logistic regression model are incapable of recovering the non-linearities introduced by the true data generating process (DGP). We consider the average log point-wise predictive density (llpd),

$$\text{llpd} = \frac{1}{n_{\text{test}}} \sum_{i=1}^{n_{\text{test}}} \log \int p(y_i^{(\text{test})} | x_i^{(\text{test})}, \theta) q_\lambda(\theta) d\theta = \frac{1}{n_{\text{test}}} \sum_{i=1}^{n_{\text{test}}} S(q_\lambda(\cdot), y_i^{(\text{test})}),$$

evaluated on a large hold-out test set with  $n_{\text{test}} = 100,000$  observations as a performance metric. Larger values indicate better predictions.

Figure 1 compares the performance of VGM-PVI for several choices of the hyperparameter  $\beta$ . The first row summarizes the posterior predictive distributions. For large  $\beta$  VGM-PVI is similar to the true posterior predictive distribution, while  $\beta = 0.01$  matches the true DGP closely. Varying  $\beta$  allows for a smooth interpolation between these two extremes. Figure 1 E) shows the llpd evaluated on the hold-out test set. The largest llpd-value is achieved by  $\beta = 0.01$ . Under this specification, VGM-PVI selects  $k = 4$  mixture components using the heuristic described above matching the four disjoint regions present in the DGP.

## 4.2 Logistic regression – Gamma telescope data

We consider a challenging classification task from astrophysics using Monte Carlo data for an imaging gamma-ray Cherenkov telescope (Bock; 2004). The goal is to discriminate

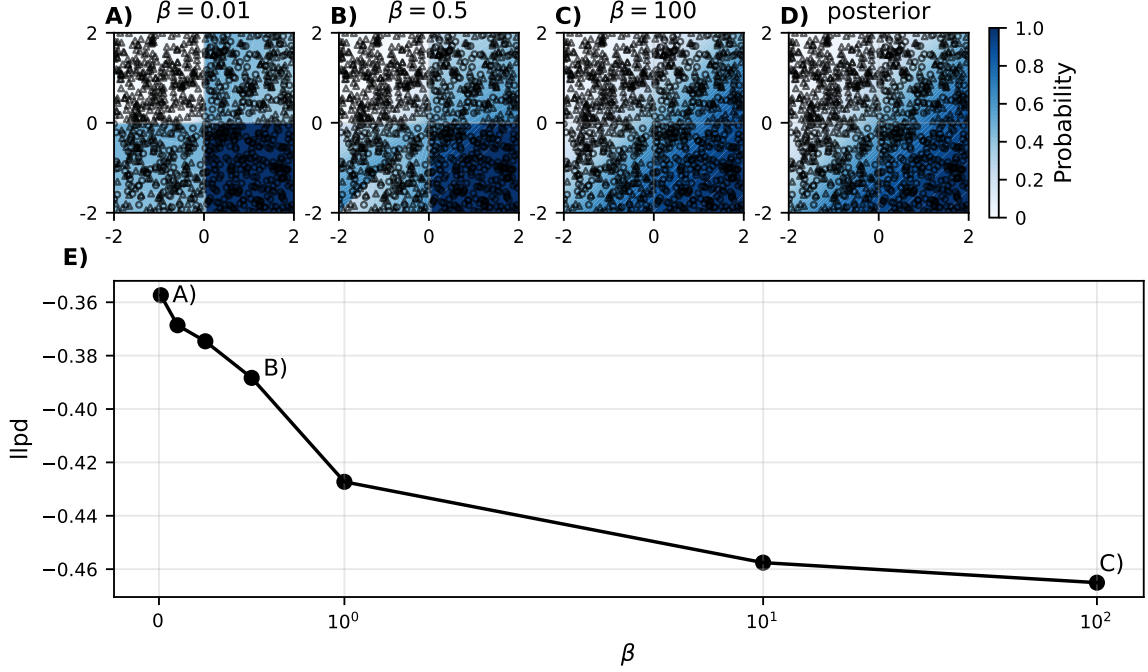


Figure 1: Simulation – Logistic regression. Posterior predictive distribution for different for **A)**  $\beta = 0.01$ , **B)**  $\beta = 0.5$ , **C)**  $\beta = 100$ , and **D)** the true posterior. The observed data is given as a scatter plot, where triangles denote  $y = 0$  and circles  $y = 1$ . **E)** plots the llpd on the hold-out test data versus different values of  $\beta$ .

observations caused by incident gamma rays (signal) from hadronic showers (noise). The data set consists of  $n = 19,020$  observations on  $d = 10$  variables summarizing the Cherenkov images. A full description of the data is given in Bock et al. (2004). As in Bock et al. (2004), we use a randomly sampled subset of  $2/3$  of the data for training and the remaining data for evaluation. The base model is a logistic regression model, where the log-odds are linked to an intercept and linear effects for all covariables. After standardisation we apply the prior  $\theta \sim \mathcal{N}(0, 2.5^2 I_{11})$ .

The receiver operating characteristic (ROC) curve on the hold-out test data is shown in Supplementary Information B.3. The ROC curve displays the true positive rate (TPR) as a function of the false positive rate (FPR) with primary gamma rays considered to be the positive class. In practice, classifying a background event as signal is worse than classifying a signal event as a hadronic shower, and therefore we are in particular interested in the TPR when the FPR is low. Table 1 reports the TPR for a number of low thresholds for the FPR. For large values of  $\beta$ , VGM-PVI performs similar to the exact posterior predictive

distribution. Decreasing  $\beta$ , however, results in a drastic improvement for out-of-sample classification for all thresholds for the FPR. VGM-PVI with a small penalty,  $\beta = 0.01$ , increases the TPR by a factor of 4 compared to the conventional posterior predictive conditional on  $\text{FPR} = 0.01$ . Earlier analyses of this data set found that classification trees and Bayes classifiers based on sophisticated density estimators are among the best performing classifiers (Bock et al.; 2004; Nagler and Czado; 2016). These methods can relate the class probabilities to complex interactions in the 10-dimensional covariate space, while a simple logistic regression model without interaction terms is incapable of modelling cross-feature dependencies. The predictive distribution resulting from VGM-PVI, (13), however, is a mixture of logistic regression models with covariate dependent weights and can thus capture some dependencies between features. This is likely the reason for the drastic increase in performance from VGM-PVI compared to the base model.

FPR	0.01	0.02	0.05	0.1	0.2
VGM-PVI ( $\beta = 0.01$ )	<b>0.3185</b>	<b>0.4029</b>	<b>0.5787</b>	<b>0.7396</b>	<b>0.8940</b>
VGM-PVI ( $\beta = 0.5$ )	0.2520	0.3549	0.5518	0.6993	0.8422
VGM-PVI ( $\beta = 1.0$ )	0.2043	0.3182	0.5161	0.6964	0.8501
VGM-PVI ( $\beta = 100$ )	0.0827	0.1717	0.3295	0.5173	0.7350
Posterior predictive	0.0775	0.1700	0.3194	0.5115	0.7271

Table 1: Gamma telescope. Comparison of TPR for a given target FPR for the hold-out test set data under both the conventional posterior predictive for the base model and different specifications of VGM-PVI with varying  $\beta$ . Bold values mark the best method per column.

### 4.3 Poisson likelihood model – AIDS case counts

To further illustrate how VGM-PVI can be helpful for model criticism and model improvement, we reanalyse quarterly counts of reported AIDS cases in the United Kingdom (UK) from January 1983 to September 1990 (Stasinopoulos and Rigby; 1992) using a Poisson GLM. The six-dimensional linear predictor consists of an intercept, a linear and a quadratic term in time, as well as binary dummy variables to capture quarterly seasonality. Due to the relatively low number of observations in this data set, a proper test-training split is infeasible. We consider therefore the widely applicable information criterion (WAIC) sug-

gested in Vehtari et al. (2017) as a model selection criterion to determine  $\beta$ . The optimal penalty parameter  $\beta^*$  is then given as

$$\beta^* = \arg \max_{\beta} \left\{ \sum_{i=1}^n \log \left( \frac{1}{M} \sum_{m=1}^M p(y_i | \theta_m) \right) - \sum_{i=1}^n V_{m=1}^M (\log(p(y_i | \theta_m))) \right\}, \quad (14)$$

where  $V_{m=1}^M(\cdot)$  is the sample variance and  $\theta_1, \dots, \theta_M \sim q_{\lambda}(\theta)$  is a sample from the variational posterior for a fixed  $\beta$ . We solve optimization problem (14) using Bayesian optimization (BO; e.g., Shahriari et al.; 2016) exploring values between 0.01 and 100. BO efficiently explores the candidate space by building a probabilistic model of the objective (14) as a function of  $\beta$ , making it a computationally attractive alternative to simple grid search.

Figure 2 A) compares the predictive distribution under the conventional posterior with that under VGM-PVI against the observed case counts. Even though a visual inspection suggests that the base model captures the data reasonably well, a small value for the penalty parameter,  $\beta \approx 0.01$ , was selected via (14) indicating that the model extension provided by VGM-PVI improves the base model. While both methods detect a similar seasonality with higher counts in the first and third quarters than in the second and fourth, the estimated temporal trends differ. Figure 2 B) shows the deseasonalised time series obtained by fixing the quarterly dummy variables at equal values. The base model yields an S-shaped temporal trend, while VGM-PVI detects an initial period of quadratic growth followed by a flattening around the beginning of 1988 before a renewed increase towards the end of the observation period. This more nuanced temporal trend matches findings in previous studies. Stasinopoulos and Rigby (1992) postulate that the introduction of antibody tests in the UK resulted in a change of behaviour for high-risk groups and consequently to a breakpoint in the temporal trend around July 1987. This dynamic cannot be captured by the linear predictor specified in the base model, a potential flaw that can be discovered by comparing the conventional posterior predictive to VGM-PVI.

## 5 PVI for hierarchical models

To illustrate how VGM-PVI can be extended to hierarchical models we analyse data on water temperature measured at a monitoring station at Upper Peirce reservoir in Singapore (Tan and Nott; 2014). The data are measured on  $n = 290$  days during the period September 9, 2010 to August 10, 2011 at  $g = 11$  different water depths from the water surface: 0.5m,

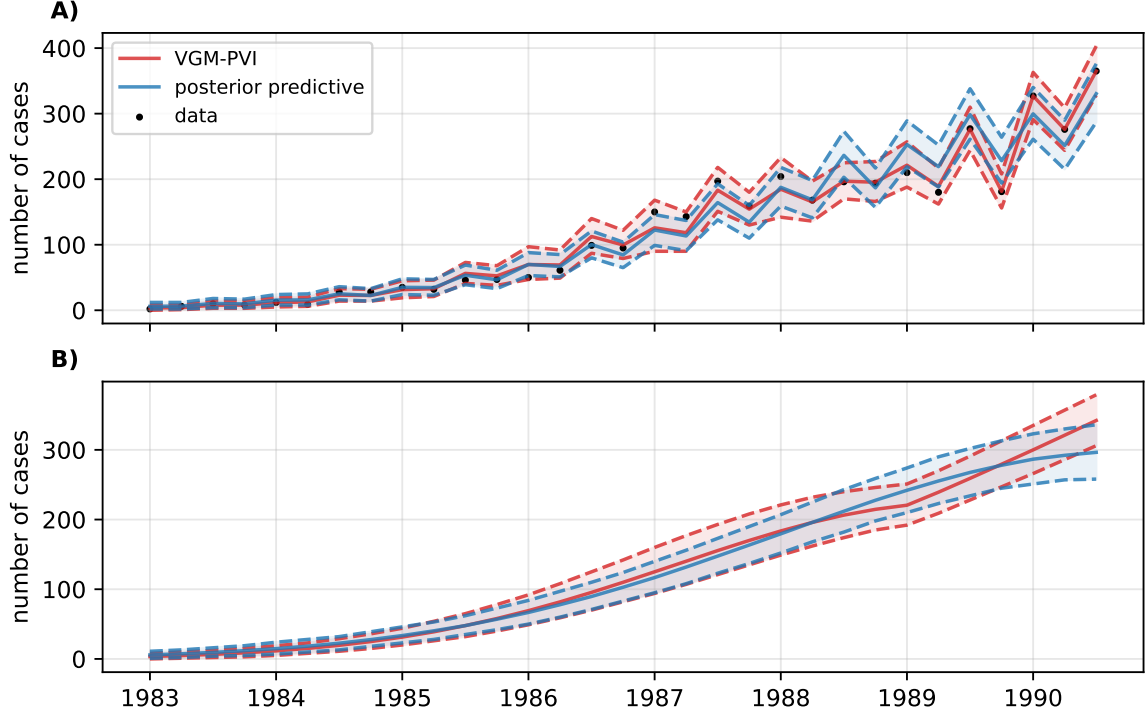


Figure 2: AIDS case counts. Panel **A)** shows the mean (bold) and a 95% credible interval (shaded) derived by VGM-PVI (red) and the true posterior (blue) as well as the observed data (points). Panel **B)** shows the deseasonalized temporal trend for both methods.

2m, 4m, 6m, 8m, 10m, 12m, 14m, 16m, 18m, and at the bottom. Writing  $y_{ij}$  for the temperature on day  $t_i$ ,  $i = 1, \dots, n$ , at depth  $j = 1, \dots, g$ , we consider a model of the form

$$y_{ij} = f(t_i) + a_i + b_j + \varepsilon_{ij}, \quad (15)$$

where  $a_i \sim \mathcal{N}(0, \sigma_a^2)$  is an observation specific random effect,  $b_j \sim \mathcal{N}(0, \sigma_b^2)$  is a random intercept for depth, and  $\varepsilon_{ij} \sim \mathcal{N}(0, \sigma_\varepsilon^2)$  represents measurement error variance. We will assume that  $\sigma_a^2, \sigma_b^2$ , and  $\sigma_\varepsilon^2$  are known. After transforming  $t \in [0, 1]$ , we model the non-linear temporal effect as  $f(t) = \beta_0 + \beta_1 t + \beta_2 t^2 + \beta_3 t^3 = x^\top \beta$  with  $x = (1, t, t^2, t^3)^\top$  and assume a weak prior  $\beta = (\beta_0, \beta_1, \beta_2, \beta_3)^\top \sim \mathcal{N}(0, 100^2)$ . Writing  $b = (b_1, \dots, b_g)^\top$  and  $a = (a_1, \dots, a_n)^\top$ , the stacked vector of unknown model parameters is  $\theta = (\beta^\top, a^\top, b^\top)^\top$ . Our interest lies in predicting a vector of water temperatures  $\tilde{y} = (\tilde{y}_1, \dots, \tilde{y}_g)^\top$  at time  $\tilde{t}$  at the previously observed water depths. For this reason, we consider a VGM-PVI of the form

$$q_\lambda(\theta|x) = \left[ \sum_{k=1}^K \omega_k(x) \phi(\theta_{\setminus a}; \mu_k, \Sigma_k) \right] \prod_{i=1}^n \phi(a_i; m_i, \tau_i^2),$$

where  $\theta_{\setminus a}$  denotes the vector of model parameters excluding the vector of observation specific intercepts  $a$ , and  $m_i, \tau_i^2, i = 1, \dots, n$  are additional variational parameters to be learned with  $\lambda$ . Then,

$$\begin{aligned} q_{\lambda}(\tilde{y} \mid \tilde{x}) &= \int \omega_k(\tilde{x}) \phi(\tilde{y}; \tilde{X} \theta_{\setminus a}, (\sigma_{\varepsilon}^2 + \sigma_a^2) I_g) \phi(\theta_{\setminus a}; \mu_k, \Sigma_k) d\theta_{\setminus a} \\ &= \sum_{k=1}^K \omega_k(\tilde{x}) \phi\left(\tilde{y}; \tilde{X}^{\top} \mu_k, \tilde{X}^{\top} \Sigma_k \tilde{X} + (\sigma_{\varepsilon}^2 + \sigma_a^2) I_g\right), \end{aligned}$$

where  $\tilde{X}$  is a stacked design matrix matching the model (15). Again, the optimal penalty parameter  $\beta^*$  is selected by optimizing the WAIC in (14). We select  $\beta^* = 0.01$ .

Figure 3 compares the observed data with the estimated mean functions  $f(t) + b_j$  for the different depths,  $j = 1, \dots, g$ , over time under VGM-PVI and the conventional posterior. The estimated mean functions have vastly different shapes. VGM-PVI results in a sharp decline between January and April that is also apparent in the data, but cannot be fully captured by the cubic polynomial the base model is restricted to. At irregular points in time aeration devices were operated to mix the water at Upper Peirce Reservoir, and it is expected that the temperature is more uniform with depth at those times. Under the base model, however, functions for different depths can only differ by a random intercept. VGM-PVI allows for more flexibility and the plot shows a clear temporal effect on the expected differences of temperature at different depths so that at least some of the heterogeneous temperature layering can be captured.

In this example, the covariate dependent mixture weights for VGM-PVI are effects of time only. VGM-PVI results therefore in an implicit clustering of time-periods and Figure 3 B) visualizes this clustering by showing  $\arg \max_k \omega_k(t)$  as a function of time. VGM-PVI selects four clusters corresponding to distinguished periods. The largest (purple) cluster corresponds to the two periods September 2010 to December 2010 and June 2011 to August 2011. In these periods VGM-PVI is closest to the conventional posterior. The second largest cluster (orange) corresponds to the period January 2011 to April 2011. In this period the water temperature plunges at all depths and VGM-PVI differs most markedly from the conventional posterior.

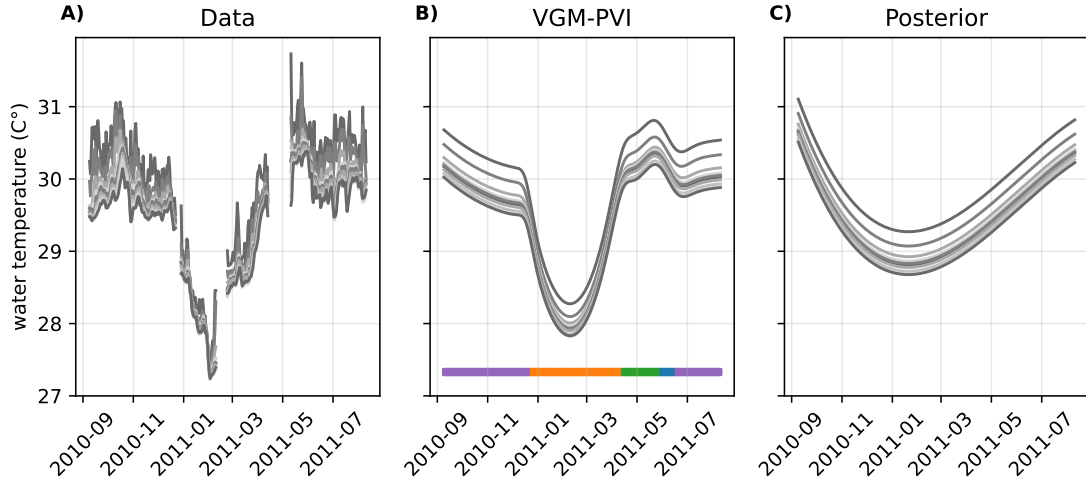


Figure 3: Temperature data. Water temperature over time at different depths (indicated by gray shades). Shown is **A)** the observed data, as well as the estimated mean functions  $f(t) + b_j$  for the different depths under **B)** VGM-PVI and **C)** the conventional posterior. **B)** also shows the dominating mixture component under VGM-PVI at each point in time (colour bar). Different clusters are indicated by colour.

## 6 PVI for latent Gaussian process models

Lastly, we consider the scenario where the likelihood term for the response  $y_i$  takes the form  $p(y_i|f(x_i))$ , depending on a latent function  $f(\cdot)$  evaluated at the covariates  $x_i$ . The latent function is given a zero mean Gaussian process prior with covariance function  $\delta(\cdot, \cdot)$ . We write  $f = (f(x_1), \dots, f(x_n))^\top$ . Dezfouli and Bonilla (2015) have considered variational inference with Gaussian mixture families for these latent GP models, and we adapt their approach here to the case of VGM-PVI. See also Bonilla et al. (2019); Fan et al. (2023) for a more detailed discussion of the approach and some extensions. Their approach is highly scalable, and uses inducing point approximations; see, for example, Quíñero-Candela and Rasmussen (2005) and Titsias (2009). Inducing point methods for GPs are related to a variety of scalable basis function approaches used in spatial statistics (Banerjee et al.; 2008; Cressie et al.; 2022).

Inducing point approximations of GPs consider an augmented posterior distribution where values of the latent process (inducing values) are considered at inducing points (covariates) denoted here by  $z_1, \dots, z_m \in \mathcal{X}$ . The introduction of the inducing points allows computations to be done using matrices of size  $m$  rather than  $n$ , where  $m \ll n$

in the case where  $n$  is large. We define  $\check{f} = (f(z_1), \dots, f(z_m))^\top$ . Henceforth we write  $X$  for the matrix with rows  $x_1, \dots, x_n$ , and  $Z$  for the matrix with rows  $z_1, \dots, z_m$ . For the posterior

$$p(f, \check{f}|y) \propto p(\check{f})p(f|\check{f})p(y|f)$$

an approximating family of the form

$$q_\lambda(f, \check{f}) = q_\lambda(\check{f})p(f|\check{f}), \quad (16)$$

is used, in which the conditional prior is used as the conditional variational posterior for  $f|\check{f}$ . By standard properties of multivariate normal distributions, the conditional prior can be expressed

$$p(f|\check{f}) = \phi(f; c, C), \quad (17)$$

where defining  $A := \delta_j(X, Z)\delta(Z, Z)^{-1}$ ,  $c = A\check{f}$  and  $C = \delta(X, X) - A\delta(Z, X)$ . Given two matrices  $X'$  and  $X''$  with rows in  $\mathcal{X}$ ,  $\delta(X', X'')$  is the matrix whose  $(k, l)$ -th entry is  $\delta(\cdot, \cdot)$  evaluated for the  $k$ -th row of  $X'$  and the  $l$ -th row of  $X''$ . For the marginal variational posterior of inducing variables, a Gaussian mixture is assumed,

$$q_\lambda(\check{f}) = \sum_{k=1}^K \omega_k \phi(\check{f}; \mu_k, \Sigma_k), \quad (18)$$

where we assume here that  $\Sigma_k$  is diagonal. From (17) and (18), we can obtain the marginal for  $f$  in (16),

$$q_\lambda(f) = \sum_{k=1}^K \omega_k \phi(f; \alpha_k, \Omega_k),$$

where  $\alpha_k = A\mu_k$  and  $\Omega_k = C - A\Sigma_k A^\top$ . In computing the ELBO and the gradient of the ELBO, we can easily obtain the marginal for  $f(x_i)$  in the above expression, and computing required expectations only requires expectations with respect to univariate marginal distributions.

To illustrate VGM-PVI for latent GP models, we consider the popular LIDAR data benchmark (Holst et al.; 1996; Ruppert et al.; 2003). The data set describes the reflection of laser-emitted light to detect chemical compounds in the atmosphere. The response variable,  $y$ , is the logarithm of the ratio of received light from two laser sources. We consider the distance travelled before the light is reflected back to its source as the only

covariate  $x$  and a Gaussian likelihood for  $y_i$ ,  $\phi(y_i; f(x_i), \sigma^2)$ . We standardize both the response and the regressor variable.

For the moment, we assume that the hyperparameter  $\sigma^2$  is fixed, and we discuss its estimation later. In this case, the predictive distribution under VGM-PVI for an unobserved  $\tilde{y}$  for observed covariate  $\tilde{x}$  is

$$q_\lambda(\tilde{y}|\tilde{x}) = \sum_{k=1}^K \omega_k(\tilde{x}) \phi(\tilde{y}; \mu(\tilde{x}), \sigma^2(\tilde{x}) + \sigma^2),$$

where

$$\begin{aligned} \mu(\tilde{x}) &= \delta(\tilde{x}, Z) \delta(Z, Z)^{-1} \mu_k \\ \sigma^2(\tilde{x}) &= \delta(\tilde{x}, \tilde{x}) - \delta(\tilde{x}, Z) \left\{ \delta(Z, Z)^{-1} - \delta(Z, Z)^{-1} \Sigma_k \delta(Z, Z)^{-1} \right\} \delta(Z, \tilde{x}). \end{aligned}$$

In PVI with the log score and the above predictive densities, prediction corresponds to plug-in prediction after fitting a mixture of experts of heteroscedastic linear models – the mean in the  $k$ th component involves predictors given by the basis functions in  $\delta(Z, Z)^{-1} \delta(Z, \tilde{x})$ , with coefficients  $\mu_k$ . For a non-Gaussian likelihood, we could use Gauss-Hermite quadrature similar to the GLM case to approximate the predictive distributions, obtaining a mixture of experts of GLMs.

A particular challenge in the LIDAR data is the pronounced heteroscedasticity, which makes it difficult to set  $\sigma^2$  upfront. Nguyen and Bonilla (2014) suggest to learn  $\sigma^2$  jointly with the variational parameters by optimizing the ELBO, and we extend this idea to VGM-PVI. To do so, we augment a component specific Dirac measure for  $\sigma^2$  independent of  $f$  into each mixture component of the variational approximation. This way,  $\sigma^2$  can vary with the covariates  $x$  through the covariate dependent weights  $\omega_k(x)$ . While Nguyen and Bonilla (2014) also learn the hyperparameters of the Gaussian process prior from the data, we consider them fixed.

The Lidar data has  $n = 221$  observations, so that we consider  $m = n$  in this application. Figure 4 plots quantile lines for the estimated predictive distribution under VGM-PVI for several choices of  $\beta$  versus the observations. For all choices of  $\beta$ , the non-linear mean function matches the data well. However, the base model cannot capture the heteroscedasticity in the data and thus for large  $\beta$  uncertainty is overestimated for small  $x$ , while smaller values of  $\beta$  capture the varying variance. For  $\beta = 0.01$ , the variance does not change gradually and an abrupt jump in uncertainty is clearly visible. This abrupt transition is inherent to

VGM-PVI as the covariate dependent mixture weights are only indirectly penalized towards smoothness in  $x$  through regularization towards the conventional posterior, and thus VGM-PVI results in a more gradual transition as  $\beta$  increases. A non-gradual transition, however, can be helpful for diagnostics as it points towards regions where the base model might be misspecified.

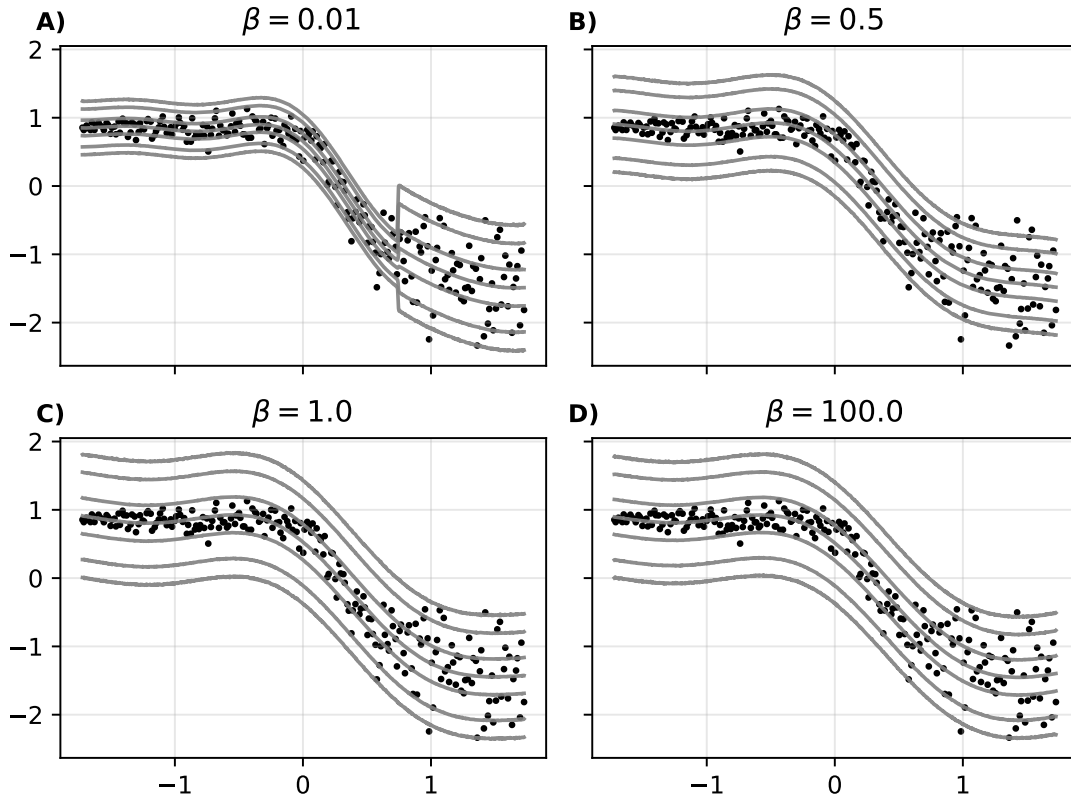


Figure 4: Lidar data. Posterior predictive distributions for **A)**  $\beta = 0.01$ , **B)**  $\beta = 0.5$ , **C)**  $\beta = 1.0$ , and **D)**  $\beta = 100$ . Gray lines correspond to quantiles at levels  $\alpha = 0.01, 0.05, 0.25, 0.5, 0.75, 0.95, 0.99$ , and the points indicate the observed data.

## 7 Discussion

We have demonstrated that PVI can be used not only to improve predictive performance under misspecification, but also to provide interpretable diagnostics that guide principled model expansions. By considering structured regression settings, we can obtain predictive distributions under GM-PVI via one-dimensional quadrature. The resulting predictive mixtures coincide with mixture-of-experts expansions of the baseline model, first with covariate-

independent weights and then, under VGM-PVI with covariate-dependent weights. The components and weights of the predictive mixture indicate where the baseline parameterization is inadequate and how parameters should vary across the covariate space to recover improved prediction in a conventional Bayesian framework.

Good performance was demonstrated in applications to linear, logistic, and Poisson regression, as well as hierarchical models with random effects, and latent Gaussian process models. In these examples, the covariate dependent weights of VGM-PVI correspond to gating functions in mixture-of-experts models, highlighting interactions, non-linearities, or non-stationarity in latent processes that the baseline model fails to capture. These factors act as diagnostic signals indicating where model expansions are most likely to be beneficial.

While the Gaussian mixture structure is highly expressive, it comes with the usual computational challenges inherent to mixture modelling: Mixture components are only identified up to permutation, and selecting an optimal number of mixture components can be challenging. Here, we proposed a simple heuristic to select a reasonable number of mixture components in a one-shot procedure jointly with learning the variational parameters. While this worked well in the examples considered, external model selection criteria might become necessary in more complex base models (e.g. Davies et al.; 2025). Our approach considered the log-score and a penalization towards the conventional posterior, but depending on the underlying task alternative scoring rules and penalizations could be explored. One merit of the log-score is that the optimization target can be derived in closed form, which allows for direct optimization of the variational parameters. Many alternative scoring rules can be written as an expectation over the variational distribution. In this case, stochastic gradient ascent, where a version of the reparametrization trick (Kingma and Welling; 2014; Rezende et al.; 2014; Xu et al.; 2019) approximates the gradient using a sample from  $q_\lambda(\theta)$ , can be used for training.

The local dependence on the covariates through the mixture weights in VGM-PVI departs from conventional Bayesian predictive inference, and a better theoretical understanding of this and the effects of different regularizers in the PVI optimization is an important direction for future research. In applications where PVI is used as a tool for model criticism, it is important that the PVI posterior has a structured form that is interpretable in terms of model expansions; although we have used Gaussian mixtures in this work, there

are other possibilities, and what is most insightful may depend on the statistical model used.

## References

- Aitchison, J. (1975). Goodness of prediction fit, *Biometrika* **62**(3): 547–554.
- Alquier, P. (2024). User-friendly introduction to PAC-Bayes bounds, *Found. Trends Mach. Learn.* **17**(2): 174–303.
- Banerjee, S., Gelfand, A. E., Finley, A. O. and Sang, H. (2008). Gaussian predictive process models for large spatial data sets, *Journal of the Royal Statistical Society Series B: Statistical Methodology* **70**(4): 825–848.
- Blei, D. M., Kucukelbir, A. and McAuliffe, J. D. (2017). Variational inference: A review for statisticians, *Journal of the American statistical Association* **112**(518): 859–877.
- Bock, R. (2004). MAGIC Gamma Telescope, UCI Machine Learning Repository. DOI: <https://doi.org/10.24432/C52C8B>.
- Bock, R. K., Chilingarian, A., Gaug, M., Hakl, F., Hengstebeck, T., Jirina, M., Klaschka, J., Kotrc, E., Savicky, P., Towers, S., Vaiciulis, A. and Wittek, W. (2004). Methods for multidimensional event classification: a case study using images from a Cherenkov gamma-ray telescope, *Nuclear Instruments and Methods in Physics Research Section A: Accelerators, Spectrometers, Detectors and Associated Equipment* **516**(2): 511–528.
- Bonilla, E. V., Krauth, K. and Dezfouli, A. (2019). Generic inference in latent Gaussian process models, *Journal of Machine Learning Research* **20**(117): 1–63.
- Chazal, C., Kanagawa, H., Shen, Z., Korba, A. and Oates, C. J. (2025). A computable measure of suboptimality for entropy-regularised variational objectives, *arXiv preprint arXiv:2509.10393*.
- Clarke, B. and Rigo, P. (2025). Introduction to the Special Issue on Contemporary Bayesian Prediction, *Statistical Science* **40**(1): 1 – 2.
- Cranmer, K., Brehmer, J. and Louppe, G. (2020). The frontier of simulation-based inference, *Proceedings of the National Academy of Sciences* **117**(48): 30055–30062.
- Cressie, N., Sainsbury-Dale, M. and Zammit-Mangion, A. (2022). Basis-function models in spatial statistics, *Annual Review of Statistics and Its Application* **9**: 373–400.

- Davies, L., MacKinlay, D., Oliviera, R. and Sisson, S. A. (2025). Transdimensional variational inference, *Advances in Neural Information Processing Systems, NeurIPS 2025*.
- Dezfouli, A. and Bonilla, E. V. (2015). Scalable inference for Gaussian process models with black-box likelihoods, in C. Cortes, N. Lawrence, D. Lee, M. Sugiyama and R. Garnett (eds), *Advances in Neural Information Processing Systems*, Vol. 28, Curran Associates, Inc.
- Evans, M. (2015). *Measuring Statistical Evidence Using Relative Belief*, Taylor & Francis.
- Fan, X., Bonilla, E. V., O’Kane, T. and Sisson, S. A. (2023). Free-form variational inference for Gaussian process state-space models, *Proceedings of the 40th International Conference on Machine Learning*, Vol. 202, PMLR, pp. 9603–9622.
- Gelman, A. and Hill, J. (2007). *Data analysis using regression and multilevel/hierarchical models*, Cambridge University Press.
- Gelman, A., Meng, X.-L. and Stern, H. (1996). Posterior predictive assessment of model fitness via realized discrepancies, *Statistica Sinica* **6**: 733–807.
- Gneiting, T. and Raftery, A. E. (2007). Strictly proper scoring rules, prediction, and estimation, *Journal of the American Statistical Association* **102**(477): 359–378.
- Hoff, P. D. and Niu, X. (2012). A covariance regression model, *Statistica Sinica* **22**(2): 729–753.
- Holst, U., Hössjer, O., Björklund, C., Ragnarson, P. and Edner, H. (1996). Locally weighted least squares kernel regression and statistical evaluation of LIDAR measurements, *Environmetrics* **7**(4): 401–416.
- Huber, M. F., Bailey, T., Durrant-Whyte, H. and Hanebeck, U. D. (2008). On entropy approximation for Gaussian mixture random vectors, *2008 IEEE International Conference on Multisensor Fusion and Integration for Intelligent Systems*, pp. 181–188.
- Jankowiak, M., Pleiss, G. and Gardner, J. (2020). Parametric Gaussian process regressors, in H. D. III and A. Singh (eds), *Proceedings of the 37th International Conference on Machine Learning*, Vol. 119 of *Proceedings of Machine Learning Research*, PMLR, pp. 4702–4712.
- Kingma, D. P. and Ba, J. (2014). Adam: A method for stochastic optimization, *arXiv preprint arXiv:1412.6980*.
- Kingma, D. P. and Welling, M. (2014). Auto-encoding variational Bayes, *2nd International*

- Conference on Learning Representations, ICLR 2014, Banff, AB, Canada, April 14-16, Conference Track Proceedings.*
- Knoblauch, J., Jewson, J. and Damoulas, T. (2022). An optimization-centric view on Bayes’ rule: Reviewing and generalizing variational inference, *Journal of Machine Learning Research* **23**(132): 1–109.
- Lai, J. and Yao, Y. (2024). Predictive variational inference: Learn the predictively optimal posterior distribution, *arXiv preprint arXiv:2410.14843* .
- Masegosa, A. (2020). Learning under model misspecification: Applications to variational and ensemble methods, in H. Larochelle, M. Ranzato, R. Hadsell, M. Balcan and H. Lin (eds), *Advances in Neural Information Processing Systems*, Vol. 33, Curran Associates, Inc., pp. 5479–5491.
- McLatchie, Y., Cherief-Abdellatif, B.-E., Frazier, D. T. and Knoblauch, J. (2025). Predictively oriented posteriors, *arXiv preprint arXiv:2510.01915* .
- Morningstar, W. R., Alemi, A. and Dillon, J. V. (2022). PACm-Bayes: Narrowing the empirical risk gap in the misspecified Bayesian regime, in G. Camps-Valls, F. J. R. Ruiz and I. Valera (eds), *Proceedings of The 25th International Conference on Artificial Intelligence and Statistics*, Vol. 151 of *Proceedings of Machine Learning Research*, PMLR, pp. 8270–8298.
- Nagler, T. and Czado, C. (2016). Evading the curse of dimensionality in nonparametric density estimation with simplified vine copulas, *Journal of Multivariate Analysis* **151**: 69–89.
- Nguyen, T. V. and Bonilla, E. V. (2014). Automated variational inference for Gaussian process models, in Z. Ghahramani, M. Welling, C. Cortes, N. Lawrence and K. Weinberger (eds), *Advances in Neural Information Processing Systems*, Vol. 27, Curran Associates, Inc.
- Ormerod, J. T. and Wand, M. P. (2010). Explaining variational approximations, *The American Statistician* **64**(2): 140–153.
- Quiñonero-Candela, J. and Rasmussen, C. E. (2005). A unifying view of sparse approximate Gaussian process regression, *Journal of Machine Learning Research* **6**(65): 1939–1959.
- Rezende, D. J., Mohamed, S. and Wierstra, D. (2014). Stochastic backpropagation and approximate inference in deep generative models, in E. P. Xing and T. Jebara (eds),

- Proceedings of the 31st International Conference on Machine Learning*, Vol. 32 of *Proceedings of Machine Learning Research*, PMLR, Beijing, China, pp. 1278–1286.
- Ruppert, D., Wand, M. P. and Carroll, R. J. (2003). *Semiparametric Regression*, Cambridge Series in Statistical and Probabilistic Mathematics, Cambridge University Press.
- Särkkä, S. and Svensson, L. (2023). *Bayesian Filtering and Smoothing (Second Edition)*, Institute of Mathematical Statistics Textbooks, Cambridge University Press.
- Shahriari, B., Swersky, K., Wang, Z., Adams, R. P. and de Freitas, N. (2016). Taking the human out of the loop: A review of Bayesian optimization, *Proceedings of the IEEE* **104**(1): 148–175.
- Shen, Z., Knoblauch, J., Power, S. and Oates, C. J. (2025). Prediction-centric uncertainty quantification via MMD, in Y. Li, S. Mandt, S. Agrawal and E. Khan (eds), *Proceedings of The 28th International Conference on Artificial Intelligence and Statistics*, Vol. 258 of *Proceedings of Machine Learning Research*, PMLR, pp. 649–657.
- Sheth, R. and Khardon, R. (2020). Pseudo-Bayesian learning via direct loss minimization with applications to sparse Gaussian process models, in C. Zhang, F. Ruiz, T. Bui, A. B. Dieng and D. Liang (eds), *Proceedings of The 2nd Symposium on Advances in Approximate Bayesian Inference*, Vol. 118 of *Proceedings of Machine Learning Research*, PMLR, pp. 1–18.
- Sisson, S., Fan, Y. and Beaumont, M. (2018). Overview of approximate Bayesian computation, in S. Sisson, Y. Fan and M. Beaumont (eds), *Handbook of Approximate Bayesian Computation*, Chapman & Hall/CRC Handbooks of Modern Statistical Methods, CRC Press, Taylor & Francis Group, Boca Raton, Florida, chapter 1.
- Stasinopoulos, D. and Rigby, R. (1992). Detecting break points in generalised linear models, *Computational Statistics & Data Analysis* **13**(4): 461 – 471.
- Tan, S. L. and Nott, D. J. (2014). Variational approximation for mixtures of linear mixed models, *Journal of Computational and Graphical Statistics* **23**(2): 564–585.
- Titsias, M. (2009). Variational learning of inducing variables in sparse Gaussian processes, in D. van Dyk and M. Welling (eds), *Proceedings of the Twelfth International Conference on Artificial Intelligence and Statistics*, Vol. 5 of *Proceedings of Machine Learning Research*, pp. 567–574.

- Vehtari, A., Gelman, A. and Gabry, J. (2017). Practical Bayesian model evaluation using leave-one-out cross-validation and WAIC, *Statistics and computing* **27**: 1413–1432.
- Walker, S. G. (2013). Bayesian inference with misspecified models, *Journal of Statistical Planning and Inference* **143**(10): 1621–1633.
- Wei, Y., Sheth, R. and Khardon, R. (2021). Direct loss minimization for sparse Gaussian processes, in A. Banerjee and K. Fukumizu (eds), *Proceedings of The 24th International Conference on Artificial Intelligence and Statistics*, Vol. 130 of *Proceedings of Machine Learning Research*, PMLR, pp. 2566–2574.
- Xu, M., Quiroz, M., Kohn, R. and Sisson, S. A. (2019). Variance reduction properties of the reparameterisation trick, *Proceedings of Machine Learning Research*, Vol. 89, AISTATS 2019.
- Yao, Y., Pirs, G., Vehtari, A. and Gelman, A. (2022). Bayesian hierarchical stacking: Some models are (somewhere) useful, *Bayesian Analysis* **17**(4): 1043 – 1071.
- Yao, Y., Vehtari, A., Simpson, D. and Gelman, A. (2018). Using stacking to average Bayesian predictive distributions (with discussion), *Bayesian Analysis* **13**(3): 917 – 1007.

## Supplementary Information

### A Analytic expression of optimization targets

This section gives analytic expressions for the optimization targets for the examples considered in the manuscript. The target of the optimization problem is

$$\begin{aligned} & \sum_{i=1}^n S(q_\lambda(\cdot), y_i) + \beta \cdot \left( \mathbb{E}_{\bar{q}_\lambda(\theta)}[\log p(y | \theta)p(\theta)] + \mathbb{E}_{\bar{q}_\lambda(\theta)}[-\log \bar{q}_\lambda(\theta)] \right) \\ = & \sum_{i=1}^n S(q_\lambda(\cdot), y_i) + \beta \cdot \left( \sum_{k=1}^K \bar{\omega}_k \left\{ \mathbb{E}_{\phi(\theta, \mu_k, \Sigma_k)}[\log p(y | \theta)] + \mathbb{E}_{\phi(\theta, \mu_k, \Sigma_k)}[\log p(\theta)] \right\} + \mathbb{E}_{\bar{q}_\lambda(\theta)}[-\log \bar{q}_\lambda(\theta)] \right). \end{aligned}$$

Approximations to the score term,  $S(q_\lambda(\cdot), y_i)$  are discussed in the manuscript directly. The entropy term,  $\mathbb{E}_{\bar{q}_\lambda(\theta)}[-\log \bar{q}_\lambda(\theta)]$  is approximated by a lower bound due to Huber et al. (2008) in all examples

$$\mathbb{E}_{\bar{q}_\lambda(\theta)}[-\log \bar{q}_\lambda(\theta)] \approx - \sum_{k=1}^K \bar{\omega}_k \log \left( \sum_{l=1}^K \bar{\omega}_l \phi(\mu_k; \mu_l; \Sigma_k + \Sigma_l) \right).$$

Terms for the expected log-likelihood,  $\mathbb{E}_{\phi(\theta, \mu, \Sigma)}[\log p(y | \theta)]$ , and for the expected log-prior  $\mathbb{E}_{\phi(\theta, \mu, \Sigma)}[\log p(\theta)]$  are model specific and we give closed form derivations for the examples considered in the manuscript below. Note that the expectation is only taken over a single mixture component  $\phi(\cdot; \mu, \Sigma)$ .

## A.1 Expected log-prior

**Independent Gaussian prior** Assume  $\theta \sim \mathcal{N}(0, \tau^2 I_p)$  with  $\tau > 0$  fixed. Then,

$$\begin{aligned} \mathbb{E}_{\phi(\theta, \mu, \Sigma)}[\log p(\theta)] &= \mathbb{E}_{\phi(\theta, \mu, \Sigma)} \left[ -\frac{p}{2} \log(2\pi\tau^2) - \frac{1}{2\tau^2} \theta^\top \theta \right] \\ &= -\frac{p}{2} \log(2\pi\tau^2) - \frac{1}{2\tau^2} \left\{ \mu^\top \mu + \text{tr} \Sigma \right\}. \end{aligned}$$

**Gaussian prior** Let  $\theta \sim \mathcal{N}(0, \Omega)$  for a known covariance matrix  $\Omega$ . Then,

$$\begin{aligned} \mathbb{E}_{\phi(\theta, \mu, \Sigma)}[\log p(\theta)] &= \mathbb{E}_{\phi(\theta, \mu, \Sigma)} \left[ -\frac{p}{2} \log(2\pi) - \frac{1}{2} \log \det \Omega - \frac{1}{2} \theta^\top \Omega^{-1} \theta \right] \\ &= -\frac{p}{2} \log(2\pi) - \frac{1}{2} \log \det \Omega - \frac{1}{2} \mu^\top \Omega^{-1} \mu + \text{tr}(\Omega^{-1} \Sigma). \end{aligned}$$

## A.2 Expected log-likelihood

**Gaussian likelihood with fixed variance** Consider the model  $y_i \sim \mathcal{N}(x_i^\top \theta, \sigma^2)$  with  $\sigma^2 > 0$  fixed. Then,

$$\begin{aligned} \mathbb{E}_{\phi(\theta, \mu, \Sigma)}[\log p(y | \theta, x)] &= \sum_{i=1}^n \mathbb{E}_{\phi(\theta, \mu, \Sigma)} \left[ -\frac{1}{2} \log(2\pi\sigma^2) - \frac{1}{2\sigma^2} (y_i - x_i^\top \theta)^2 \right] \\ &= -\frac{n}{2} \log(2\pi\sigma^2) - \frac{1}{2\sigma^2} \sum_{i=1}^n \left\{ (y_i - x_i^\top \mu)^2 + x_i^\top \Sigma x_i \right\} \end{aligned}$$

**Linear regression with unknown variance** We consider  $y_i \sim \mathcal{N}(x_i^\top \beta, \sigma^2)$ , where  $\theta = (\beta^\top, \log \sigma^2)^\top$  is the stacked vector of model parameters. Write  $\tau = \log \sigma^2$ .

First, consider the term  $\mathbb{E}_{\phi(\theta, \mu, \Sigma)}[\log p(y | \theta, x)]$ . We can decompose

$$\mu = \begin{pmatrix} \mu_\beta \\ \mu_\tau \end{pmatrix} \quad \text{and} \quad \Sigma = \begin{pmatrix} \Sigma_{\beta\beta} & \Sigma_{\beta\tau} \\ \Sigma_{\tau\beta} & \Sigma_{\tau\tau} \end{pmatrix}$$

We note that under  $\theta \sim \mathcal{N}(\mu, \Sigma)$  we can write  $\beta | \tau$  as a normal distribution with mean

$\mu_{\beta|\tau}(\tau) = \mu_\beta + \Sigma_{\beta\tau}\Sigma_{\tau\tau}^{-1}(\tau - \mu_\tau)$  and covariance  $\Sigma_{\beta|\tau} = \Sigma_{\beta\beta} - \Sigma_{\beta\tau}\Sigma_{\tau\tau}^{-1}\Sigma_{\tau\beta}$ . Then,

$$\begin{aligned}\mathbb{E}_{\phi(\theta,\mu,\Sigma)}[\log p(y | \theta, x)] &= \sum_{i=1}^n -\frac{1}{2} \log(2\pi) - \frac{1}{2} \mathbb{E}_{\phi(\theta,\mu,\Sigma)}[\tau] - \frac{1}{2} \mathbb{E}_{\phi(\theta,\mu,\Sigma)}[\exp(-\tau)(y_i - x_i^\top \beta)^2] \\ &= -\frac{n}{2} \log(2\pi) - \frac{n}{2} \mu_\tau - \frac{1}{2} \sum_{i=1}^n \mathbb{E}_{\phi(\theta,\mu,\Sigma)}[\exp(-\tau)(y_i - x_i^\top \beta)^2] \\ &= -\frac{n}{2} \log(2\pi) - \frac{n}{2} \mu_\tau - \frac{1}{2} \exp(-\mu_\tau + \frac{1}{2} \Sigma_{\tau\tau}) \sum_{i=1}^n \left\{ (y_i - x_i^\top (\mu_\beta - \Sigma_{\beta\tau}))^2 + x_i^\top \Sigma_{\beta\beta} x_i \right\}.\end{aligned}$$

Similarly for the score term,

$$\begin{aligned}\int \phi(\tilde{y}; \tilde{x}^\top \beta, \sigma^2) \phi(\theta; \mu, \Sigma) d\theta &= \int \int \phi(\tilde{y}; \tilde{x}^\top \beta, \sigma^2) \phi(\beta; \mu_{\beta|\tau}(\tau), \Sigma_{\beta|\tau}) d\beta \phi(\tau; \mu_\tau, \Sigma_{\tau\tau}) d\tau \\ &= \int \phi(\tilde{y}; \tilde{x}^\top \mu_{\beta|\tau}(\tau), \tilde{x}^\top \Sigma_{\beta|\tau} \tilde{x} + \exp(\tau)) \phi(\tau; \mu_\tau, \Sigma_{\tau\tau}) d\tau \\ &= \int \phi(\tilde{y}; \tilde{x}^\top \mu_{\beta|\tau}(\mu_\tau + \sqrt{\Sigma_{\tau\tau}} w), \tilde{x}^\top \Sigma_{\beta|\tau} \tilde{x} + \exp(\mu_\tau + \sqrt{\Sigma_{\tau\tau}} w)) \phi(w; 0, 1) dw \\ &\approx \sum_{b=1}^B \gamma_b \phi\left(\tilde{y}; \tilde{x}^\top \mu_{\beta|\tau}\left(\mu_\tau + \sqrt{\Sigma_{\tau\tau}} w_b\right), \tilde{x}^\top \Sigma_{\beta|\tau} \tilde{x} + \exp\left(\mu_\tau + \sqrt{\Sigma_{\tau\tau}} w_b\right)\right),\end{aligned}$$

where  $w_b$  and  $\gamma_b$  are Gauss-Hermite quadrature points and weights respectively. We have  $\mu_{\beta|\tau}(\mu_\tau + \sqrt{\Sigma_{\tau\tau}} w_b) = \mu_\beta + \Sigma_{\beta\tau} \sqrt{\Sigma_{\tau\tau}}^{-1} w_b$ .

**Poisson regression** Under the Poisson model  $y_i | \theta \sim Pois(\exp(x_i^\top \theta))$  we have

$$\begin{aligned}\mathbb{E}_\phi(\theta; \mu, \Sigma) [\log p(y | \theta)] &= \sum_{i=1}^n \mathbb{E}_\phi(\theta; \mu, \Sigma) \left[ y_i x_i^\top \theta - \exp(x_i^\top \theta) - \log(y_i!) \right] \\ &= \sum_{i=1}^n y_i x_i^\top \mu - \exp(x_i^\top \mu + \frac{1}{2} x_i^\top \Sigma x_i) - \log(y_i!).\end{aligned}$$

**Logistic regression** Consider a logistic regression model

$$\mathbb{P}(y_i = 1) = \frac{1}{1 + \exp(-x^\top \theta)}.$$

Then we approximate

$$\begin{aligned}\mathbb{E}_{\phi(\theta,\mu,\Sigma)}[\log p(y | \theta)] &= \sum_{i=1}^n \mathbb{E}_{\phi(\theta,\mu,\Sigma)} \left[ y_i \log \frac{1}{1 + \exp(-x^\top \theta)} + (1 - y_i) \log \left( 1 - \frac{1}{1 + \exp(-x^\top \theta)} \right) \right] \\ &\approx \sum_{b=1}^B \gamma_b \left[ y_i \log \frac{1}{1 + \exp(-x^\top \mu - w_b x_i^\top \Sigma x_i)} \right. \\ &\quad \left. + (1 - y_i) \log \left( 1 - \frac{1}{1 + \exp(-x^\top \mu - w_b x_i^\top \Sigma x_i)} \right) \right],\end{aligned}$$

where  $w_b$  and  $\gamma_b$  are Gauss-Hermite quadrature points and weights respectively.

## B Additional experiments

### B.1 Simulations – Linear regression

We generate  $n = 1,000$  observations as

$$y_i \sim \mathcal{N}(x_i^3, \sigma^2),$$

where the  $x_i$  are uniform on  $[-2, 2]$ . To this data we fit the misspecified linear regression model

$$\begin{aligned} y_i &= \theta_1 + x_i \theta_2 + \varepsilon_i \\ \varepsilon_i &\sim \mathcal{N}(0, \sigma^2) \\ \theta &\sim \mathcal{N}(0, \tau^2 I_2), \end{aligned}$$

where  $\sigma^2 = 0.1$  and  $\tau^2 = 100$  are known. We vary the tuning parameters  $\beta$  for VGM-PVI and evaluate the predictive performance using the lpd on an additional hold-out test set with  $n_{\text{test}} = 10,000$ .

From previous discussion we know that for large values of  $\beta$ , VGM-PVI converges towards the true posterior predictive distribution, and that VGM-PVI matches the true DGP for small values of  $\beta$ . This is in-line with findings in Lai and Yao (2024). Figure 5 A) compares the predictive distribution under VGM-PVI for the optimal value  $\beta^* = 0.01$  with the predictive distribution under the true posterior. The true posterior is incapable of capturing the non-linear relationship between  $x$  and  $y$  resulting in an unfavourable prediction model. In contrast to this, VGM-PVI is a covariate dependent mixture of linear models resulting in a piecewise linear approximation to the non-linear regression function. In particular, VGM-PVI identifies 3 regions in the covariate space and fits separate linear models to the data within each region. This can be seen by an investigation of the mixture weights given in Figure 5 B). For all values of  $\beta$  only a small number of mixture components is selected. In particular for large  $\beta$  only a single component is selected, which is expected as the true posterior is a single Gaussian distribution. For the optimal value  $\beta^* = 0.01$ , VGM-PVI selects three mixture components. Their activity corresponds to the kinks in the mean function of the DGP resulting in interpretable weights.

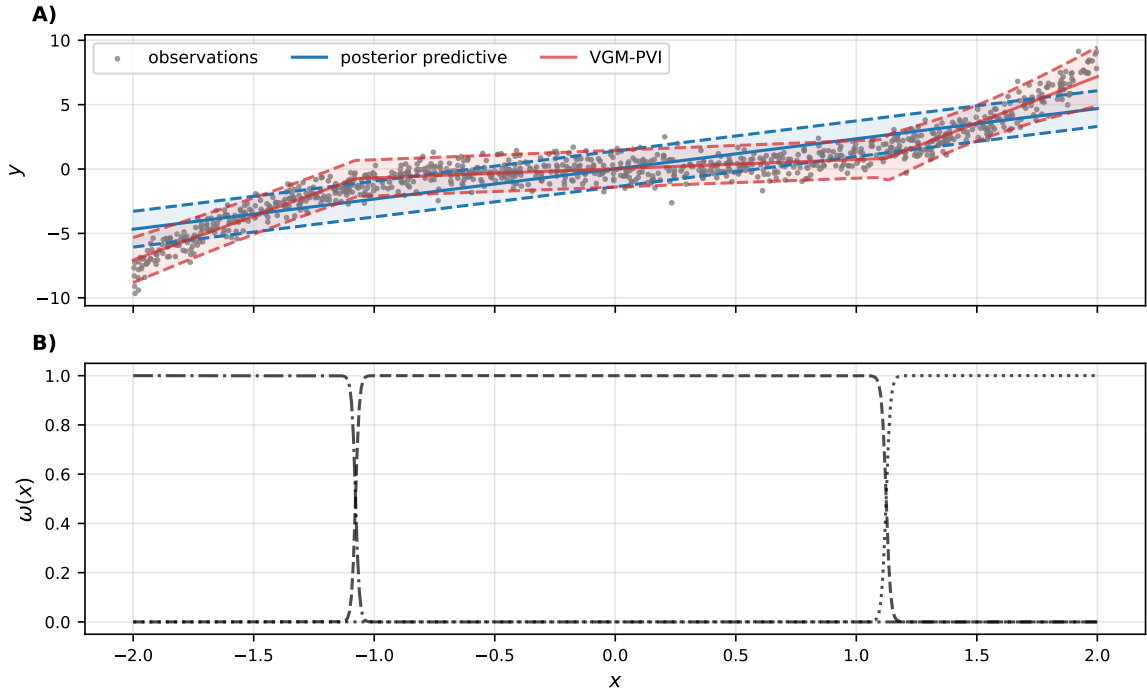


Figure 5: Simulation – Linear regression. Panel **A)** shows the mean (bold) and a 95% credible interval (dashed) derived by VGM-PVI under  $\beta = 0.01$  (red) and the true posterior (blue). Panel **B)** shows the behaviour of the weights  $\omega_k(x)$  under VGM-PVI. Different weights are differentiated by line-style.

## B.2 Gaussian likelihood model – IQ data

This example illustrates PVI for a Gaussian likelihood model with potentially unknown variance. The dataset contains cognitive test scores of  $n = 434$  three and four-year-old children (Gelman and Hill; 2007). The response variable is the child’s IQ  $q_i$ , and we have the mother’s IQ,  $m_i$ , as well as a binary indicator indicating whether or not the mother completed high school,  $h_i$ , as covariables. After converting the IQ score to Z-scores, we consider the likelihood model

$$q_i \sim \mathcal{N}(\theta_0 + \theta_1 h_i + \theta_2 m_i, \sigma^2),$$

where we assume a prior  $\theta = (\theta_0, \theta_1, \theta_2)^\top \sim \mathcal{N}(0, I_3)$ . In addition to a full Bayesian approach we also consider two plug-in estimators,  $\hat{\sigma}^2 = \sigma_1^2, \sigma_2^2$ , for  $\sigma^2$  as this gives additional insight in the model extension provided by VGM-PVI. Explicitly,  $\hat{\sigma}^2 = \sigma_1^2 = (n - 3)^{-1} \sum_{i=1}^n (q_i - \hat{q}_{i,\text{LQE}})^2$ , where  $\hat{q}_{i,\text{LQE}}$  is the predicted value under the least squares estimator for  $\theta$ ,  $i = 1, \dots, n$ . Also,  $\hat{\sigma}^2 = \sigma_2^2 = 0.05\sigma_1^2$ , so that the base model is bound to under-

	$\sigma^2 = \sigma_1^2$		$\sigma^2 = \sigma_2^2$		$\log \sigma^2 \sim \mathcal{N}(0, 1)$	
	OUT-llpd	IN-llpd	OUT-llpd	IN-llpd	OUT-llpd	IN-llpd
VGM-PVI	-147.0766	-542.9843	-494.2149	-1750.8228	-154.2008	-560.5294
Posterior predictive	-149.1583	-547.825	-810.4417	-3203.3109	-149.2536	-547.8748

Table 2: IQ data. llpd evaluated on the trainings data (IN-llpd), and the test data (OUT-llpd) for VGM-PVI and the conventional posterior predictive.

estimate uncertainty. For the fully Bayesian approach, we assume the prior  $\log \sigma^2 \sim \mathcal{N}(0, 1)$  and  $\log \sigma^2$  becomes an additional model parameter, so that  $\theta = (\theta_0, \theta_1, \theta_2, \log \sigma^2)^\top$  in this case. We consider a randomly sampled subset of 80% of the data for training and selection of  $\beta$ , while the remaining 20% of the data are used for evaluation. Again, we select the optimal VGM-PVI by optimizing (14) via BO. Table 2 reports both the in-sample and the out-sample llpd for all three scenarios.

For  $\hat{\sigma}^2 = \sigma_1^2$ , VGM-PVI improves the conventional posterior only slightly, while we observe much greater improvement in the severely misspecified case  $\hat{\sigma}^2 = \sigma_2^2$ . In the third case, the conventional posterior performs better than VGM-PVI for both in- and out-sample predictions.

### B.3 Additional results: Gamma telescope data

Figure 6 shows the ROC curve for the Gamma telescope example. VGM-PVI improves on the base model for all values of  $\beta$ . For  $\beta = 100$ , VGM-PVI performs similar to the posterior, while the best performance is achieved for  $\beta = 0.01$ .

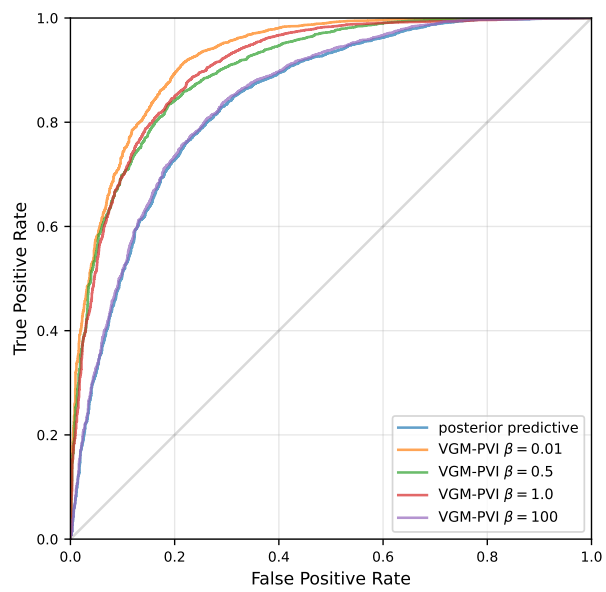


Figure 6: Gamma telescope. ROC curves on the hold-out test data for the conventional posterior and VGM-PVI with  $\beta = 0.01, 0.05, 1.0, 100$  (indicated by colour).